

DRA

EE-SSL-1802

EE-SSL-1802

## Interim Report

# SKYLAB NEUTRON ENVIRONMENT EXPERIMENT [SCIENCE DEMONSTRATION SD-34 (TV108)]

## DESCRIPTION AND PRELIMINARY RESULTS

April 1974

N74-35237

(NASA-CR-120446) SKYLAB NEUTRON  
ENVIRONMENT EXPERIMENT (SCIENCE  
DEMONSTRATION SD-34 (TV108)) . . . DESCRIPTION  
AND PRELIMINARY RESULTS (Teledyne Brown  
Engineering) 24 p HC \$4.25 CSCL 03B

Unclass  
17128  
G3/30



# BROWN ENGINEERING

Cummings Research Park • Huntsville, Alabama 35807

INTERIM REPORT  
EE-SSL-1802

SKYLAB NEUTRON ENVIRONMENT EXPERIMENT  
[SCIENCE DEMONSTRATION SD-34 (TV108)]

DESCRIPTION AND PRELIMINARY RESULTS

By

G. J. Fishman, Ph.D.

April 1974

Prepared For

SPACE SCIENCES LABORATORY  
GEORGE C. MARSHALL SPACE FLIGHT CENTER  
HUNTSVILLE, ALABAMA

Contract No. NAS8-26342

Prepared By

ELECTRONICS AND ENGINEERING  
TELEDYNE BROWN ENGINEERING  
HUNTSVILLE, ALABAMA

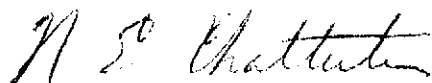
## ABSTRACT

Neutron and proton induced radioactivity at various locations within Skylab were measured. Samples of five metals were formed into activation packets and deployed at the following locations on the Skylab IV mission:

- Orbital Workshop film vault
- Water storage tank
- Two opposing Orbital Workshop internal locations.

Radioactive nuclides were produced in the packets by nuclear interactions of high-energy protons and secondary neutrons within Skylab. Low-level gamma-ray spectroscopy measurements were made on the returned packets to determine the incident neutron and proton fluxes and spectra and their variations with mass distribution.

Approved:



---

N. E. Chatterton, Ph.D.  
Manager  
Research Laboratories

## TABLE OF CONTENTS

|                               | Page |
|-------------------------------|------|
| INTRODUCTION . . . . .        | 1    |
| ACTIVATION SAMPLES . . . . .  | 2    |
| GAMMA-RAY ANALYSIS . . . . .  | 7    |
| PRELIMINARY RESULTS . . . . . | 8    |
| FURTHER ANALYSIS . . . . .    | 17   |

# LIST OF ILLUSTRATIONS

| Figure | Title   | Page |
|--------|---|------|
| 1      | Skylab IV Activation Packets . . . . .                                      | 4    |
| 2      | Deployed Activation Packets - Skylab IV . . . .                             | 6    |
| 3      | Gamma-Ray Spectrum - Packet No. 2 . . . . .                                 | 10   |
| 4      | Gamma-Ray Spectra - Four Packets and<br>Background Control Packet . . . . . | 11   |
| 5      | Buildup and Decay of Activation Isotopes . . . .                            | 13   |
| 6      | Activation of Nickel and Titanium . . . . .                                 | 15   |
| 7      | Activation of Tantalum by Neutrons . . . . .                                | 16   |

## LIST OF SYMBOLS

|                      |   |
|----------------------|---|
| $A_m$                | Measured activity   |
| $A_{sat}$            | Saturated activity  |
| $A_{t_0}$            | Activity at end of mission  |
| $B(E)$               | Gamma-ray branching ratio   |
| $D_{sat}$            | Disintegration rate at saturation                                   |
| $f(\Delta t)$        | Correction factor due to decay during measuring interval $\Delta t$ |
| $N_A$                | Avagadro's number = $6.02 \times 10^{23}$                           |
| $(n, p)$             | Nuclear reaction, indicating neutron capture and proton ejection    |
| $P(E)$               | Detector photopeak efficiency                                       |
| $S(E)$               | Self-absorption factor of sample                                    |
| $t_1$                | Time in orbit = 84.0 days   |
| $t_2$                | Time after de-orbit   |
| $\bar{\sigma}$       | Average cross section   |
| $\tau_{\frac{1}{2}}$ | Half-life   |
| $\phi(E)$            | Differential energy flux  |
| $\Phi(E_1 - E_2)$    | Integral flux between $E_1$ and $E_2$                               |

## INTRODUCTION

Large, orbiting spacecraft are expected to produce significant numbers of neutrons through nuclear reactions between trapped protons and spacecraft materials. While measurements of upward-moving atmospheric neutrons (the neutron albedo) have been studied, a systematic study of locally produced, secondary neutrons in spacecraft has not yet been made. Although secondary neutrons have previously been shown to contribute a negligible dose to astronauts, their great penetrating power and ability to activate many materials may seriously degrade the sensitivity of X-ray and gamma-ray detectors on orbiting spacecraft. This is especially true of scintillation and solid-state detectors aboard the High-Energy Astronomy Observatory spacecraft. For these detectors, prompt, charged-particle-produced background can be greatly reduced by active shielding, whereas there is no known method of reducing activation background in the detectors.

The Skylab Neutron Environment Science Demonstration measured neutrons and protons by the activation analysis technique. In this technique, samples of known compositions were exposed to the unknown neutron and proton environment at various locations within Skylab. After return of the samples, they were analyzed in a low-level, high-resolution gamma-ray spectrometer to deduce the type and amount of radioactive isotopes produced during their irradiation. The neutron and proton environments can then be derived by using the appropriate activation cross sections.

The author is grateful to Dr. T. A. Parnell for initiating this experiment and to Messrs. Tom Bannister and Larry Russell for their help with the flight preparations and operations. The Skylab Corollary Experiments support personnel were also of great assistance.

## ACTIVATION SAMPLES

Four activation sample packets were flown and returned on the Skylab IV mission. They were deployed by the crew at the locations within the Orbital Workshop (OWS) given in Table 1. The four activation sample packets each contained five samples of high-purity metals, with dimensions of 1.91 by 1.91 by 0.32 centimeters. Four of the metal samples were tantalum, nickel, titanium, and hafnium. The fifth sample was tantalum with a covering layer of 0.65-millimeter-thick cadmium, which excluded thermal neutrons. The cadmium had a minimum absorption length of seven mean-free paths for neutrons with energies less than 0.2 eV. The samples were sewn into beta cloth (fiberglass) to form the activation packets as shown in Figure 1. Table 2 indicates the properties of the samples.

The activation packets were in the Skylab IV orbit for the mission duration (November 16, 1973 to February 5, 1974). During the initial 5.3 days and the final 2.7 days of the mission, the packets were stowed in a Command Module locker. The remainder of the time, 76.0 days or 91 percent of the orbital time, the packets were deployed at the locations given in Table 1 and shown in Figure 2.



TABLE 1. ACTIVATION PACKET LOCATIONS

| PACKET       | LOCATION   | SHIELDING -- RADIATION ENVIRONMENT EXPECTED  |
|--------------|--|--|
| 1-FV         | OWS Film Vault, Drawer J                                 | Maximum shielding -- secondary neutrons, few protons                               |
| 2-WT         | Water Storage Tank (Full), OWS, Taped on Outside of Tank | Moderate shielding -- thermalized neutrons   |
| 3-OWS<br>FWD | OWS Forward -- Taped on Domed Bulkhead                   | Average shielding -- near center of mass of Skylab cluster                         |
| 4-OWS<br>AFT | OWS Aft -- Taped on Outside Wall in Sleep Compartment    | Minimum shielding for internal location -- few secondary neutrons, maximum protons |



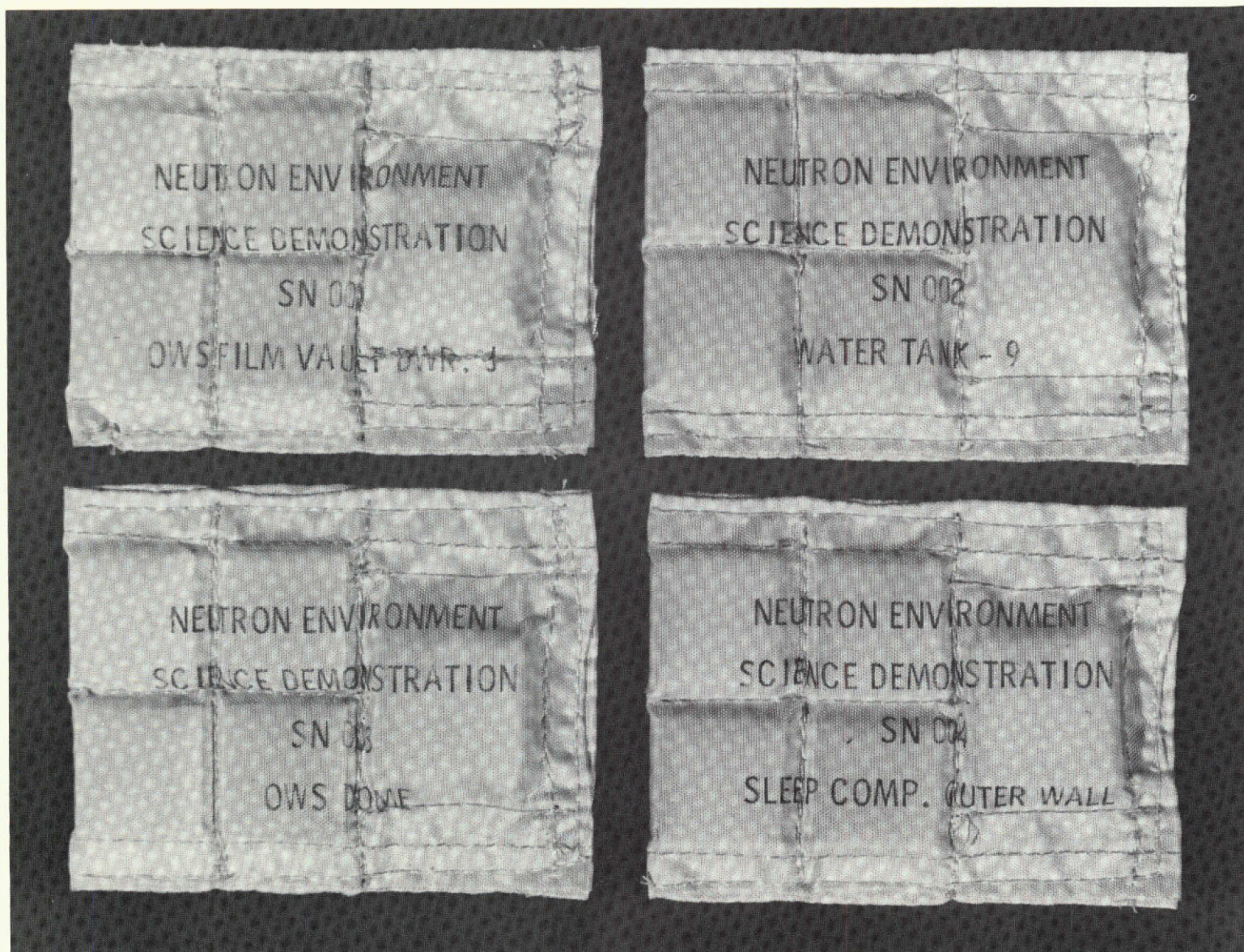
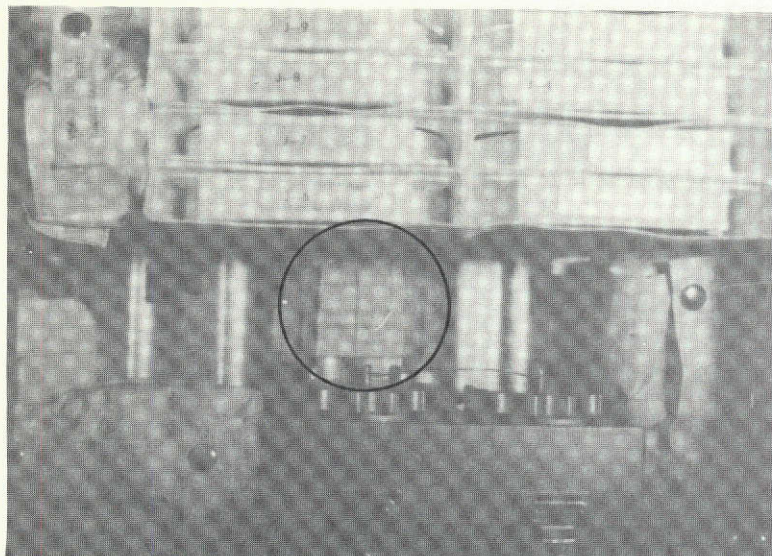


FIGURE 1. SKYLAB IV ACTIVATION PACKETS. Five metal activation samples were sewn into each packet (shown approximately actual size).

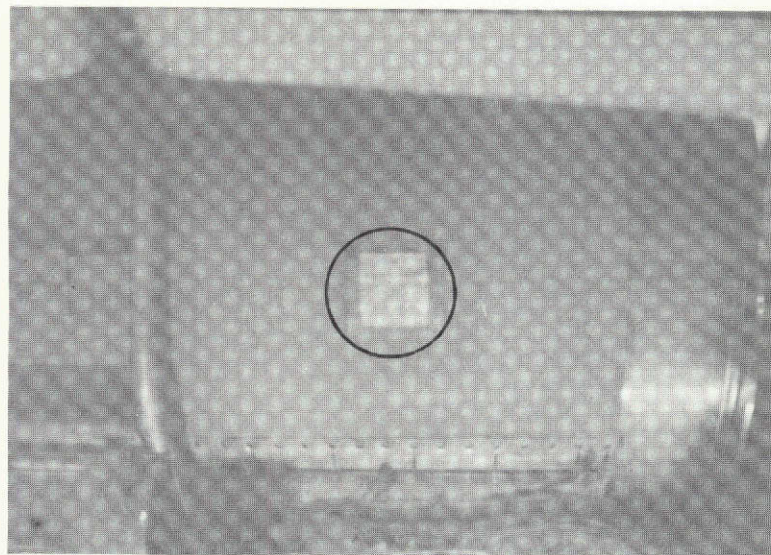


TABLE 2. ACTIVATION SAMPLES

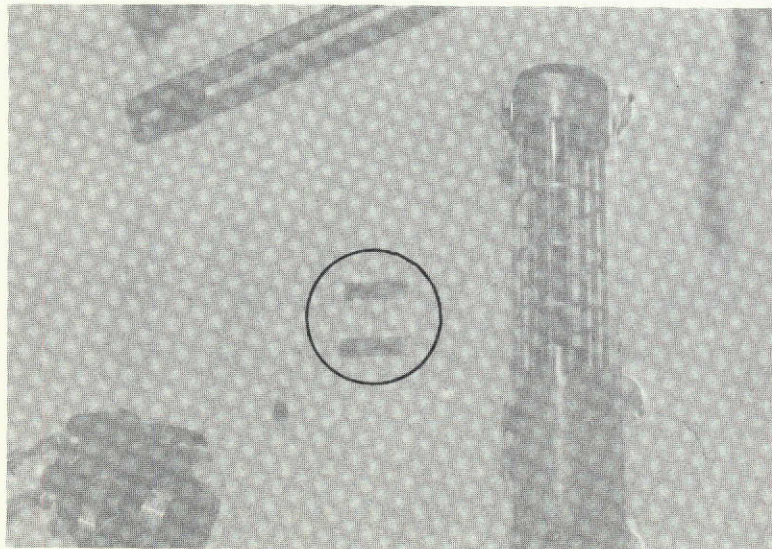
| SAMPLE                        | NOMINAL<br>WEIGHT (grams) | MAIN<br>ISOTOPES  |
|-------------------------------|---------------------------|---|
| 1. Tantalum (bare)            | 19                        | Ta <sup>181</sup> (100%)  |
| 2. Tantalum (cadmium-wrapped) | 19                        | Ta <sup>181</sup> (100%)  |
| 3. Nickel                     | 12                        | Ni <sup>58</sup> (68%), Ni <sup>60</sup> (26%)  |
| 4. Titanium                   | 5.6                       | Ti <sup>48</sup> (74%), Ti <sup>46</sup> (8%),<br>Ti <sup>47</sup> (7%)                               |
| 5. Hafnium                    | 17                        | Hf <sup>180</sup> (35%), Hf <sup>179</sup> (14%),<br>Hf <sup>178</sup> (27%), Hf <sup>177</sup> (19%) |



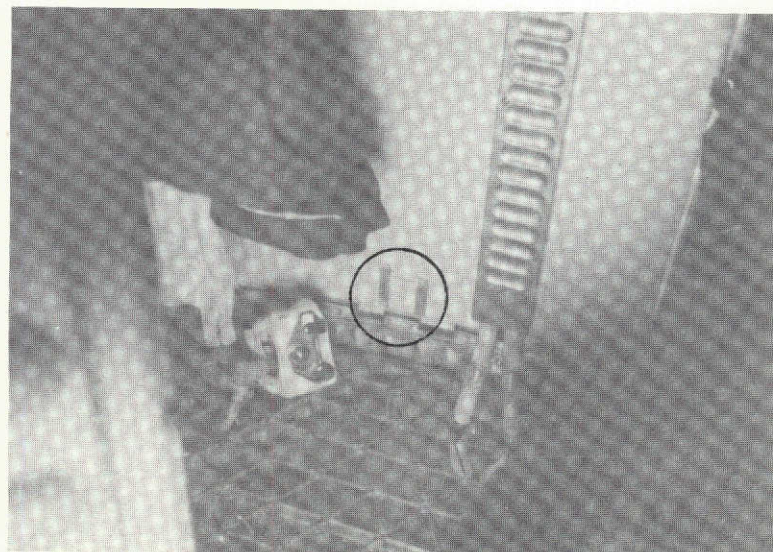
FILM VAULT



WATER TANK



OWS FWD



OWS AFT

FIGURE 2. DEPLOYED ACTIVATION PACKETS - SKYLAB IV



## GAMMA-RAY ANALYSIS

A low-level gamma-ray spectrometer system was assembled in the Space Sciences Laboratory of George C. Marshall Space Flight Center to analyze the Skylab activation samples. The detector is a high-efficiency, lithium-drifted, germanium diode with a nominal volume of 80 cubic centimeters. The system resolution is typically 2.5 keV at 1.33 MeV over a 5-day counting period. Considerable effort was made to reduce the background and keep it constant. The facility was isolated in a small room with thick concrete walls. A lead shield with a minimum thickness of 20 centimeters surrounded about 90 percent of the detector head and the remaining solid angle was shielded by a minimum of 10 centimeters of lead. A 1.3-centimeter-thick copper shield was used to reduce the amount of lead fluorescence X-rays, produced near the surface of the lead shield, which entered the detector. Spectra are recorded by a 1024-channel PHA and stored on digital magnetic tape. Spectral dispersions are from 1.0 to 1.5 keV per channel.

## PRELIMINARY RESULTS

The radioactive isotopes which have been found in the returned samples, along with their nuclear decay properties and production modes, are listed in Table 3. All activities found were extremely weak; the average count rate for a particular isotope was less than one count per hour. The initial set of gamma-ray measurements on each packet was made with counting times of 400,000 seconds (4.63 days). One such spectrum is shown in Figure 3, where the induced radionuclide gamma-ray lines are indicated. All other lines in the spectrum, as well as the continuum, are part of the measured background. Most of the background radiation is due to terrestrial activity (thorium, uranium, and radioactive daughter products) in the soil and concrete building materials which penetrate the lead shielding of the detector.

Figure 4 shows the higher energy portions of all four sample packets and a background spectrum taken with a control sample packet that was not flown. Gamma-ray lines found in the background are indicated by numbers.

Quantitative measurements of the activation peak intensities were made by subtracting a symmetric average of the adjacent background continuum, yielding an activity,  $A_m$ . One activation line, the 1121-keV line of  $Ta^{182}$ , coincided with a background line from  $Bi^{214}$ . The strength of the background line was determined and subtracted out. The activity of each isotope was then corrected to yield the saturation activity,  $A_{sat}$ , through the formula

$$A_{sat} = \frac{A_m \times f(\Delta t)}{\frac{A_m}{A_{t_0}} \times \frac{A_{t_0}}{A_{sat}}}$$

TABLE 3. ACTIVATION ISOTOPES IDENTIFIED

| ISOTOPE                      | $\tau_{1/2}$ (DAYS) | $E_{\gamma}$ (keV)           | PRODUCTION MODES                 |  |
|------------------------------|---------------------|------------------------------|----------------------------------|--|
|                              |                     |                              | MAIN                             | OTHER  |
| Co <sup>58</sup>             | 71                  | 810                          | Ni <sup>58</sup> (n,p)           | Ni(p,2pxn), Ni(n,pxn)  |
| Ta <sup>182</sup>            | 115                 | 1121<br>1189<br>1222<br>1231 | Ta <sup>181</sup> (n, $\gamma$ ) |  |
| Co <sup>56</sup>             | 77                  | 847                          | Ni <sup>58</sup> (p,2pn)         | Ni(p,2pxn), Ni(n,pxn), Ni(p,pxn)Ni <sup>56</sup> , Ni(n,xn) Ni <sup>56</sup> |
| Co <sup>57</sup>             | 270                 | 122                          | Ni <sup>58</sup> (p,2p)          | Ni(p,2pxn), Ni(n,pxn), Ni(n,xn)Ni <sup>57</sup>                              |
| V <sup>48</sup>              | 16                  | 983                          | Ti <sup>48</sup> (p,n)           |  |
| OTHER IDENTIFICATIONS (WEAK) |                     |                              |                                  |  |
| Sc <sup>46</sup>             | 84                  | 889                          | Ti(p,-)                          |  |
| Lu <sup>171</sup>            | 8.3                 | 741                          | Hf(p,-)                          | Ta(p,-)  |
| Hf <sup>175</sup>            | 70                  | 343                          | Hf(p,-)                          | Ta(p,-)  |

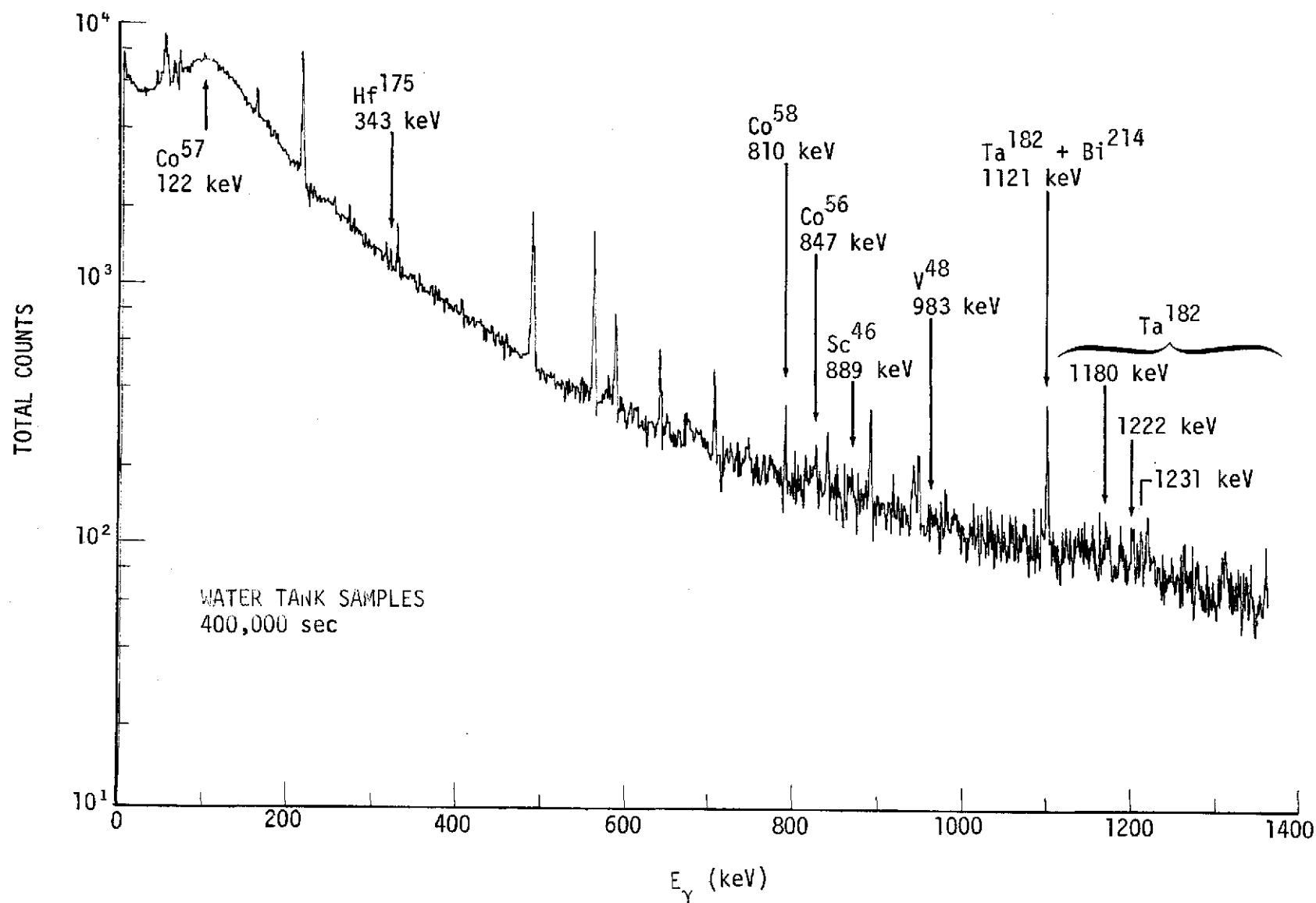


FIGURE 3. GAMMA-RAY SPECTRUM - PACKET NO. 2. The activation gamma-ray peaks are identified; all other peaks are due to background gamma-ray lines. A strong background continuum is also apparent.



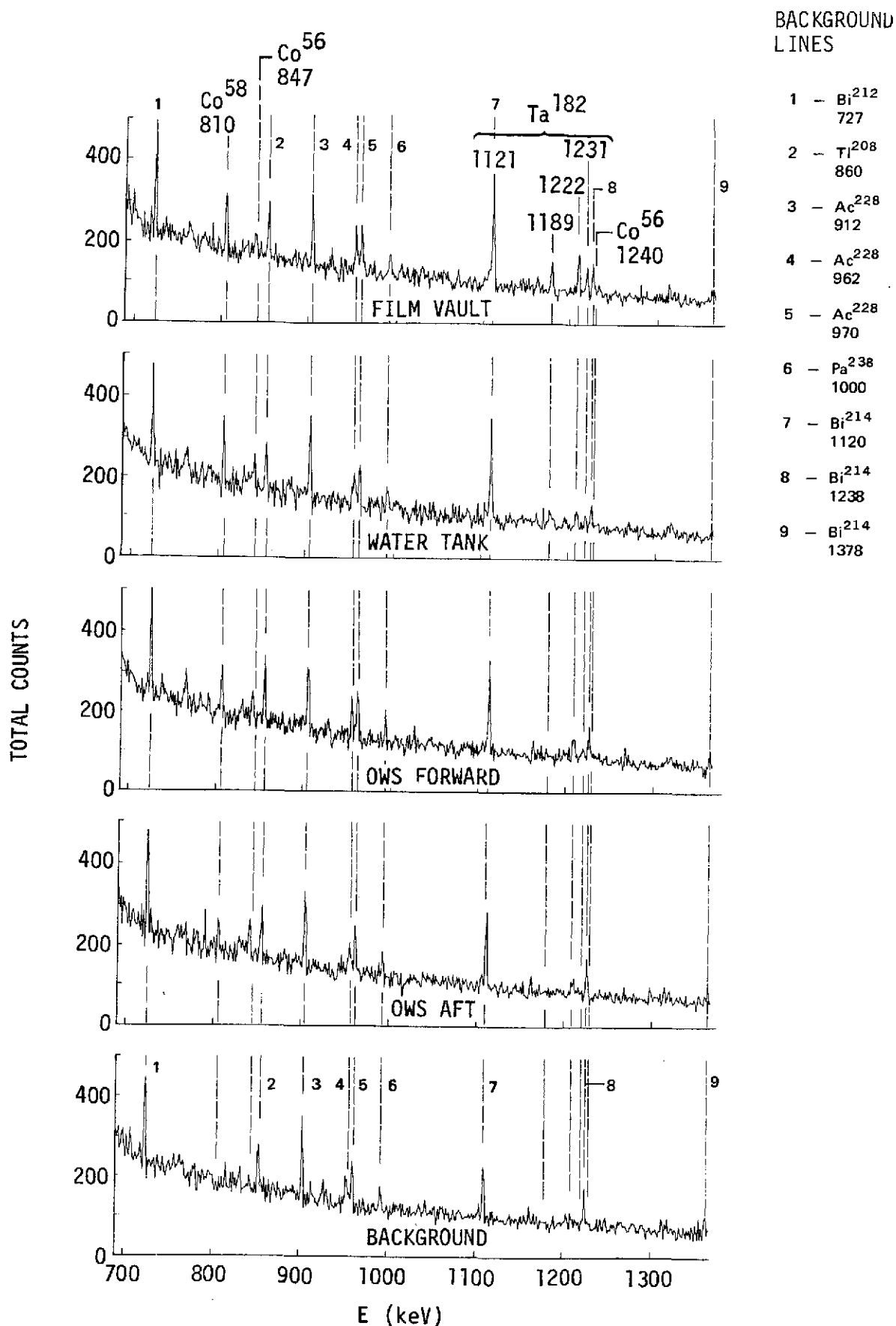


FIGURE 4. GAMMA-RAY SPECTRA - FOUR PACKETS AND BACKGROUND CONTROL PACKET. Peaks due to background gamma-ray lines are indicated by numbers. Note the differences in activation peak intensities for the four packets. Decay corrections described in the text have not been applied to these raw count-rate spectra.

where  $A_{t_0}$  is the activity at the end of the mission and  $A'_m$  is the instantaneous activity at the start of the activity measuring interval,  $\Delta t$ . The quantity  $f(\Delta t) = \frac{A'_m}{A_m}$  is a correction factor which accounts for decay during the activity counting time,  $\Delta t$ , and is given by the following equation:

$$f(\Delta t) = \frac{\Delta t \ln 2}{\tau_{\frac{1}{2}}} \times \frac{1}{1 - \exp\left(\frac{-\Delta t \ln 2}{\tau_{\frac{1}{2}}}\right)} .$$

For most cases,  $f(\Delta t) \approx 1$  since  $\Delta t \ll \tau_{\frac{1}{2}}$ .

The quantities,  $A_{t_0} / A_{sat}$  and  $A'_m / A_{t_0}$ , correct for the buildup of the isotope during the mission and the decay afterwards, respectively:

$$\frac{A_{t_0}}{A_{sat}} = 1 - \exp(-t_1 \ln 2 / \tau_{\frac{1}{2}})$$

and

$$\frac{A'_m}{A_{t_0}} = \exp\left(-t_2 \ln 2 / \tau_{\frac{1}{2}}\right)$$

where  $t_1$  is the time in orbit,  $t_2$  is the time after de-orbit, and  $\tau_{\frac{1}{2}}$  is the half-life of the particular isotope. Figure 5 shows the buildup and decay for five of the identified isotopes. The quicker buildup and decay of the shorter lived isotopes is apparent.

The saturated activity for each gamma ray line was then corrected for the Ge(Li) detector photopeak efficiency,  $P(E)$ ; for the gamma-ray branching ratio,  $B(E)$ ; and for self-absorption in the sample,  $S(E)$ . The saturated disintegration rate,  $D_{sat}$ , was derived according to

$$D_{sat} = \frac{A_{sat}}{B(E) \times P(E) \times S(E)} .$$

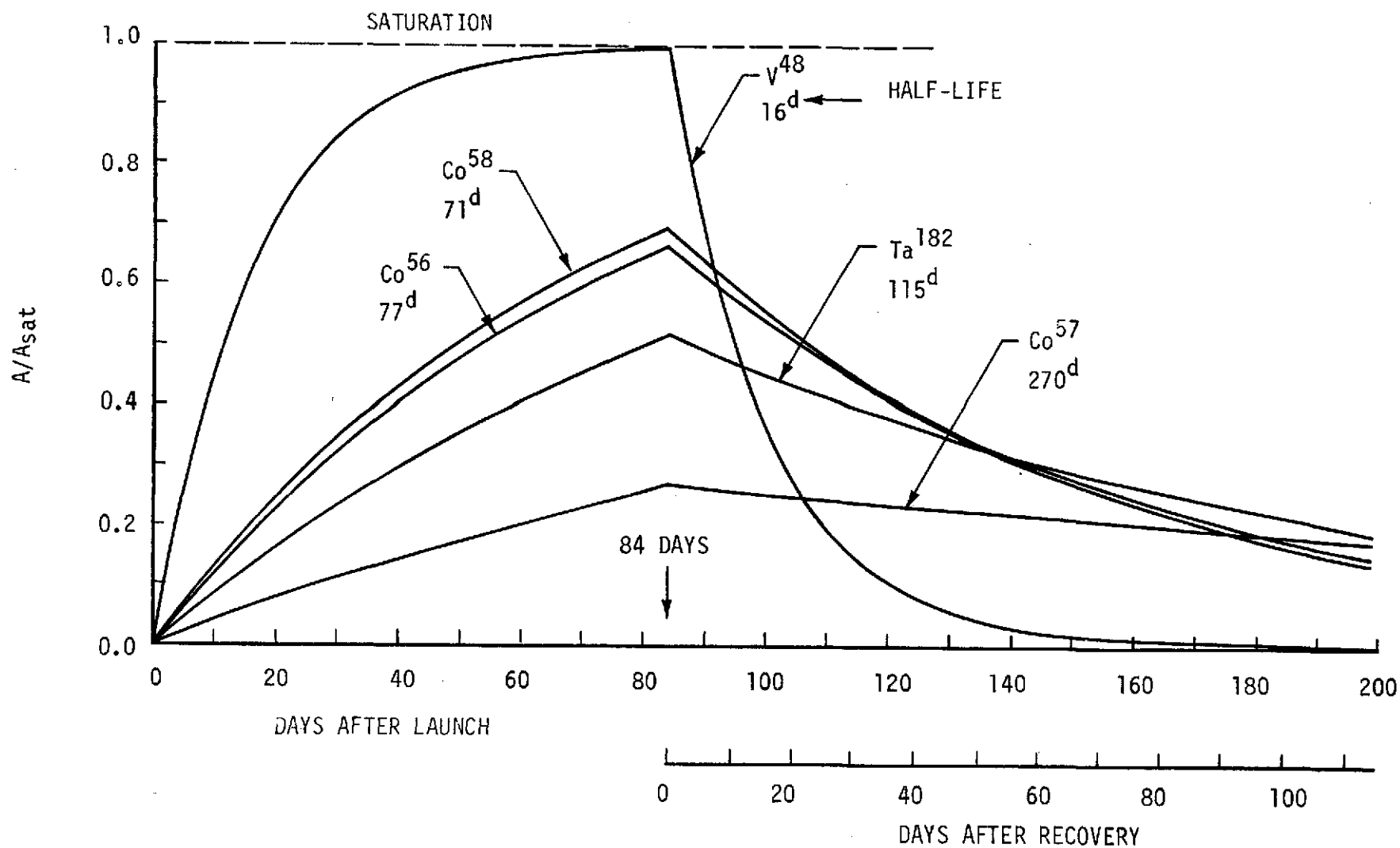


FIGURE 5. BUILDUP AND DECAY OF ACTIVATION ISOTOPES

The normalized disintegration rates for various isotopes produced at the four Skylab locations are given in Figures 6 and 7. Each data point represents an independent measurement of a particular gamma-ray line counted for 400,000 seconds. The error bars associated with each measurement are due only to statistical errors. These errors are believed to be greater than any systematic errors in the measurements.

These preliminary measurements (Figures 6 and 7) show that both neutron and proton activation isotopes were produced in the samples from which several qualitative observations can be made:

- $\text{Co}^{58}$ , which has a high-yield cross section from  $\text{Ni}^{58}$  via the fast neutron (n, p) reaction, is produced in greater quantity in the higher mass locations.
- $\text{Co}^{56}$  and  $\text{V}^{48}$ , which are proton activation products of nickel and titanium, respectively, are produced at the lower mass locations.  $\text{Co}^{57}$  shows no clear enhancement.
- $\text{Ta}^{182}$ , a neutron capture product, is produced more at the higher mass locations. The capture cross section rises rapidly at thermal neutron energies. The lack of enhancement at the water tank location probably indicates a low thermal to fast neutron flux ratio. Measurements of the cadmium-wrapped tantalum, not yet made, should indicate the thermal neutron component.
- Proton activation in the film vault location, as evidenced by  $\text{Co}^{56}$  and  $\text{V}^{48}$ , indicates the presence of the high-energy tail of trapped protons and/or primary galactic cosmic rays. Some of this activation could be due to temporary storage of the packet while in the Command Module.

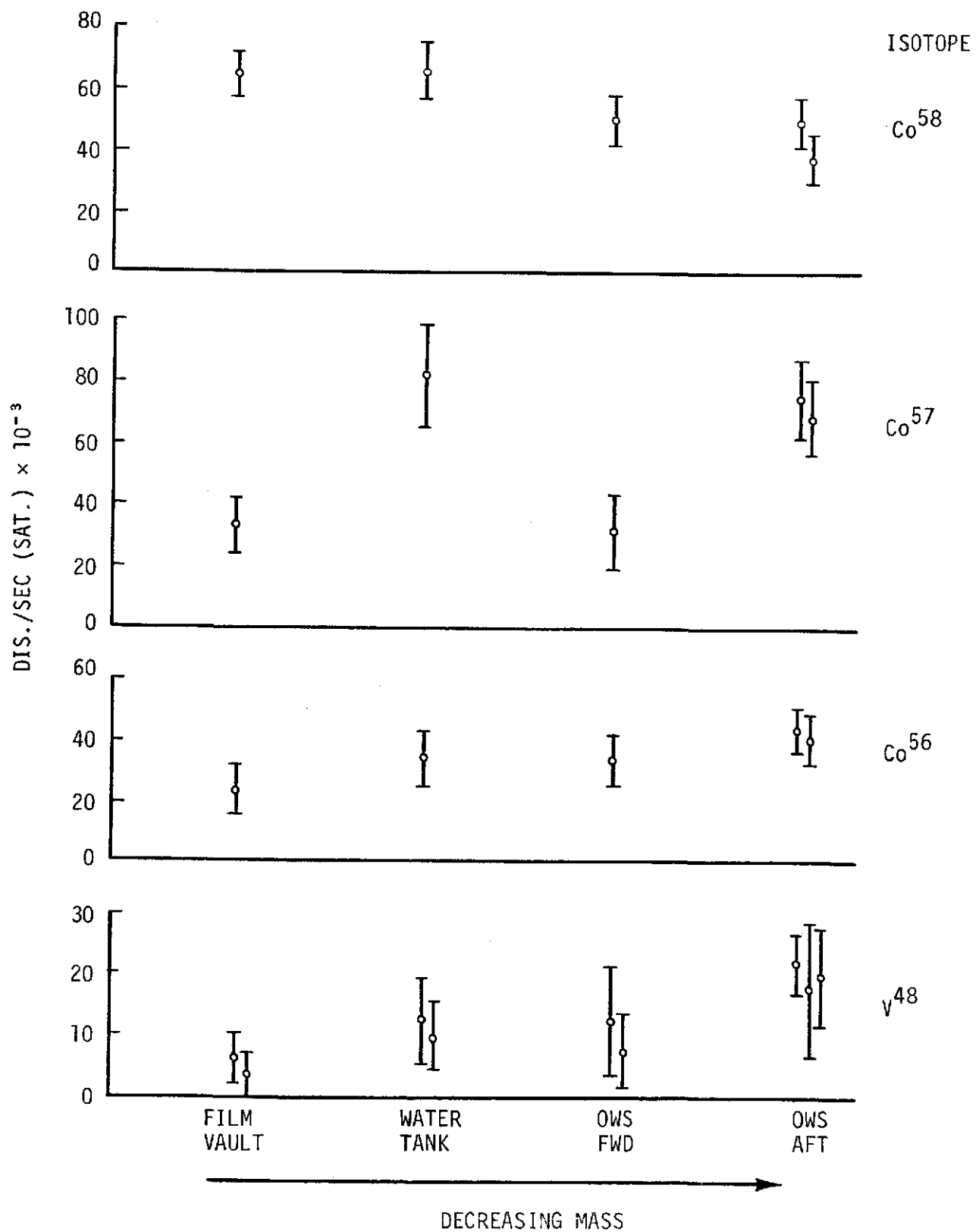


FIGURE 6. ACTIVATION OF NICKEL AND TITANIUM

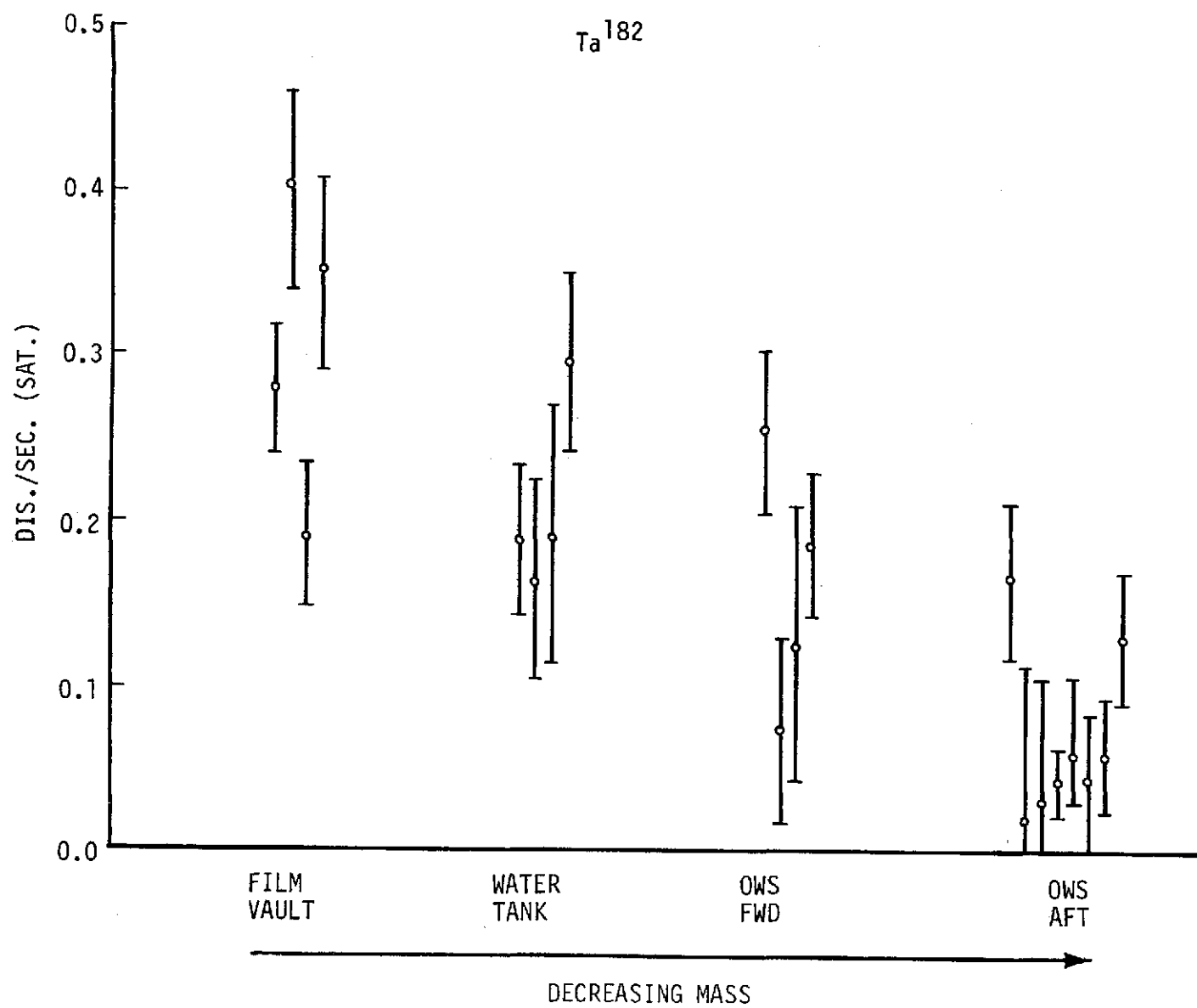


FIGURE 7. ACTIVATION OF TANTALUM BY NEUTRONS

## FURTHER ANALYSIS

The preliminary activation results presented in the previous section will be improved upon as more measurements are made. However, the ultimate quantities to be measured are the incident neutron and proton fluxes. The differential neutron and proton fluxes,  $\phi(E)$ , are related to the saturated disintegration rate,  $D_{\text{sat}}$ , through the formula

$$D_{\text{sat}} = \frac{N_A M}{A} \int \phi(E) \sigma(E) dE$$

where

$N_A$  - Avagadro's Number

$M$  - mass of sample

$A$  - atomic weight of sample

$\sigma(E)$  - cross section for activation.

In theory,  $\phi(E)$  may be unfolded from a set of independent equations of the type above by using one of the iterative computer codes that have been developed for this application. For the present Skylab measurements, we are limited in the number of activation species so that the usual unfolding programs would not give meaningful results. Instead, the integral flux,  $\Phi(E_1 - E_2)$ , over the energy interval,  $E_1$  to  $E_2$ , is evaluated by assuming a differential spectral shape of arbitrary intensity,  $\phi'(E)$  and using a mean cross section,  $\bar{\sigma}$ .

Then

$$\Phi(E_1 - E_2) = \frac{A D_{\text{sat}}}{N_A M \bar{\sigma}}$$

where

$$\bar{\sigma} = \frac{\int_{E_1}^{E_2} \phi'(E) \sigma(E) dE}{\int_{E_1}^{E_2} \phi'(E) dE} .$$

Both proton and neutron spectral forms have been calculated for various mass thicknesses in orbiting spacecraft. Initially, these fluxes will be used to derive the integral fluxes. If the integral fluxes from different species do not agree in the same energy ranges, the assumed spectral form will be modified and the calculations repeated to give better agreement. In this manner, deviations from the assumed spectral form may be found.

This analysis will be made in the near future when more accurate disintegration measurements become available from longer counting intervals. A compilation of the appropriate activation cross sections is now in progress. A rough, order-of-magnitude calculation shows that the neutron fluxes will be from 0.5 to 5/cm<sup>2</sup> sec. This flux is comparable to the high-energy proton flux. While, of course, the measurements have no time resolution, almost all of the flux is received during passages through the South Atlanta anomaly. The time-averaged neutron activation for certain materials is greater than proton activation in most spacecraft locations.